Effect of Preloading on the Contact Stress Distribution of a Dovetail Interface

Kaliyaperumal Anandavel, Raghu V. Prakash and Antonio Davis

Abstract—This paper presents the influence of preloading on a) the contact tractions, b) slip levels and c) stresses at the dovetail blade-disc interface of an aero-engine through a three-dimensional (3D) finite element (FE) modeling and analysis. The preloading is applied by an interference fit at the dovetail interface and the bulk loading is applied through the rotational speed of rotor. Preloading at the dovetail interface reduces the peak contact pressure developed due to bulk loading up to 35%, and reduces the peak contact pressure and stress difference between top and bottom contact edges. Increasing the level of preloading reduces the cyclic stress amplitude at the interface up to certain values of preload and as a consequence, an improvement in fatigue life could be expected. Fretting damage, due to vibration and wind milling effect during engine ground condition, can be minimized by preloading the dovetail interface.

Keywords—Dovetail interface, Preload, Interference fit, Contact Stress, Fretting Fatigue.

I. INTRODUCTION

AN aero-engine fan and compressor rotor design involves dovetail interface between the blade and the disc. The blade-disc interface is an important element in the rotor assembly, as premature crack initiation [1] occurs due to fretting damage at this interface that results in catastrophic rotor failures. Incorporating the fretting aspects in the design system of dovetail interface would improve the rotor design, and satisfy the requirements of a lighter engine, with better performance without any compromise on the safety. The blade dovetail loosely fits [2], [3] in the compressor disc until the rotor spins and the centrifugal forces push the blade dovetail firmly and radially upward against the dovetail slot in the disc. The easy insertion and removal of fan blades from the attachment requires a radial small space between bottom of dovetail root of blade and corresponding slot surface of disc. However, when the engine is not operating, the fan blades are free to slowly rotate or likely to experience windmill due to wind or breezes on the ground at the airport. Preloads are applied on the fan blade with a radial outward force to eliminate wear between blade root and the dovetail slot during wind milling conditions, by introducing a spacer or wedge

Kaliyaperumal Anandavel is a Ph.D. Research Scholar with Indian Institute of Technology Madras, Chennai, India and working with Infotech Enterprises Ltd., Bangalore, India. (e-mail: Anandavel.Kaliyaperumal@infotech-enterprises.com)

Raghu V. Prakash is with Department of Mechanical Engineering, Indian Institute of Technology Madras, Chennai, India. (Corresponding author phone: +91-44-2257 4694; fax: +91-44-2257 4652; e-mail: raghuprakash@iitm.ac.in).

Antonio Davis is with Infotech Enterprises Ltd., Bangalore, India. (E-mail: Antonio.Davis@infotech-enterprises.com).

between blade root bottom and disc slot.

Tsai et al. [4] analyzed the effect of pre-stress on a strip of specimen using finite element analysis. Boddington et al. [5] developed two-dimensional elastic analysis FE code which had the modeling capability to include the relative motion and friction at the interface. This code was used in the two-dimensional fretting fatigue investigation [6]. Meguid et al. [7] carried out two-dimensional finite element contact analysis of dovetail interface for predicting overall stress distribution. Sinclair et al. [8] demonstrated that the conforming contact stresses at the dovetail interface is non-singular (for friction and non-friction cases) through an asymptotic analysis; finite element analysis of dovetail attachment should produce stress convergence through selection of a fine mesh at the interface. Their mesh refinement study with sub-modeling approach in two-dimensional analysis has shown that the interface element size of one percent of local or nearby fillet radius (R) is required to achieve five percent stress convergence. Hammouda et al. [9] have carried out 2D finite element contact analysis to predict probable fretting fatigue crack in the dovetail interface.

Papanikos et al. [10] have shown that 3D geometric effect plays significant role in increasing contact edge stress at compressor dovetail and turbine fir-tree interfaces using 3D finite element contact analysis, though the mesh refinement level in these analysis appears to be not adequate enough to capture the converged peak stresses. Beisheim et al. [11] implemented three-dimensional sub-modeling for obtaining converged contact edge stress at dovetail interface, using standard commercial code ANSYS ®. The 3D elastic analysis has been carried out only for frictionless contact model.

The two-dimensional and three-dimensional analysis [5]-[11] of dovetail does not consider the preloading effect in the analysis. The preload application by introducing spacer or wedge between blade root bottom and disc slot, results in additional fretting zones on the blade and disc. Hence the current study considers introducing interference fit at the blade-disc interface itself, as this will avoid additional fretting zones in the blade-disc dovetail assembly. The objective of present study is to explore and understand the influence of preload on the contact traction, slip and contact stresses which are the major contributing factors for fretting damage [12] at the dovetail interface. The study is carried out on skewed dovetail for (a) preload at the interface and (b) combined preload and bulk load due to angular velocity. The three-dimensional finite element study has been carried out, using

ANSYS three-dimensional finite element contact [13] capabilities.

II. THREE-DIMENSIONAL FE MODELING AND ANALYSIS

A. FE Modeling

The current study considers the dovetail configuration as used in [10]. The geometric details and dimensions of the dovetail are shown in Fig. 1(a). Dovetail assembly with a skew angle of 20° configuration is used for this study, as the skew angle has significant impact on the contact pressure and stresses. 3D FE modeling is developed for global and sub-modeling analysis, using eight node solid elements (ANSYS SOLID45). Surface to surface contact elements (ANSYS - TARG170 and CONTAC173) are deployed for modeling the interface of dovetail attachment, using standard unilateral contact. Coulomb's friction model in [13] is employed at the interface.

The global model is analyzed with the cyclic symmetric boundary conditions imposed on the sector faces of the disc, with the assumption of cyclic symmetry loading on the rotor. One node on the disc, away from the contact interface, is constrained in the axial and tangential direction of the global model to prevent rigid body motion. One node on the blade is also constrained in axial direction. Six weak springs, with a stiffness of 5 N/mm, are used to connect the blade and disc in the global model. The FE details of global model are shown in Fig. 1(b).

Sub-modeling is implemented for one side of the interface as shown in Fig. 1(c), with finer level of mesh refinement. Mesh refinement is implemented up to R/h= 160 (R is the nearest fillet edge radius, h is the contact element size in radial direction) with aspect ratios of 2 and 4 in tangential and axial direction respectively, at the contact edges of sub-model. Displacements are chosen as quantities to be taken from global model analysis results, for use in boundary conditions of sub-model grids, as it helps for faster solution convergence. Contact elements of varying sizes are used at the interface, and a local coordinates system used for interface results analysis is shown in Fig. 1(d). The contact model uses combined algorithm (Lagrange in normal and penalty in shear contact) for contact solution of dovetail interface. Details of variational formulation and finite element implementation procedures of contact algorithms are available in [14].

B. Analysis

Elastic analysis with contact non-linearity is carried out in this study, at a uniform temperature of 300K. Material properties of the Ti-alloy (Young's modulus = 110 GPa, Poisson's ratio: 0.3, Density: 4500 kg/m^3) are used in this study. Analysis is carried out for a friction coefficient of 0.3. SPARSE solver is used with 1% force convergence tolerance in this non-linear analysis. Sensitivity studies are carried out on the global model and sub-model for a various number of sub-steps used in the nonlinear solving process. Based on this sensitivity study, a minimum of 50 and five sub-steps are

defined for all the analysis of global and sub models respectively. Analyses are carried out for different combinations of interference fits and bulk load as indicated in Table I.
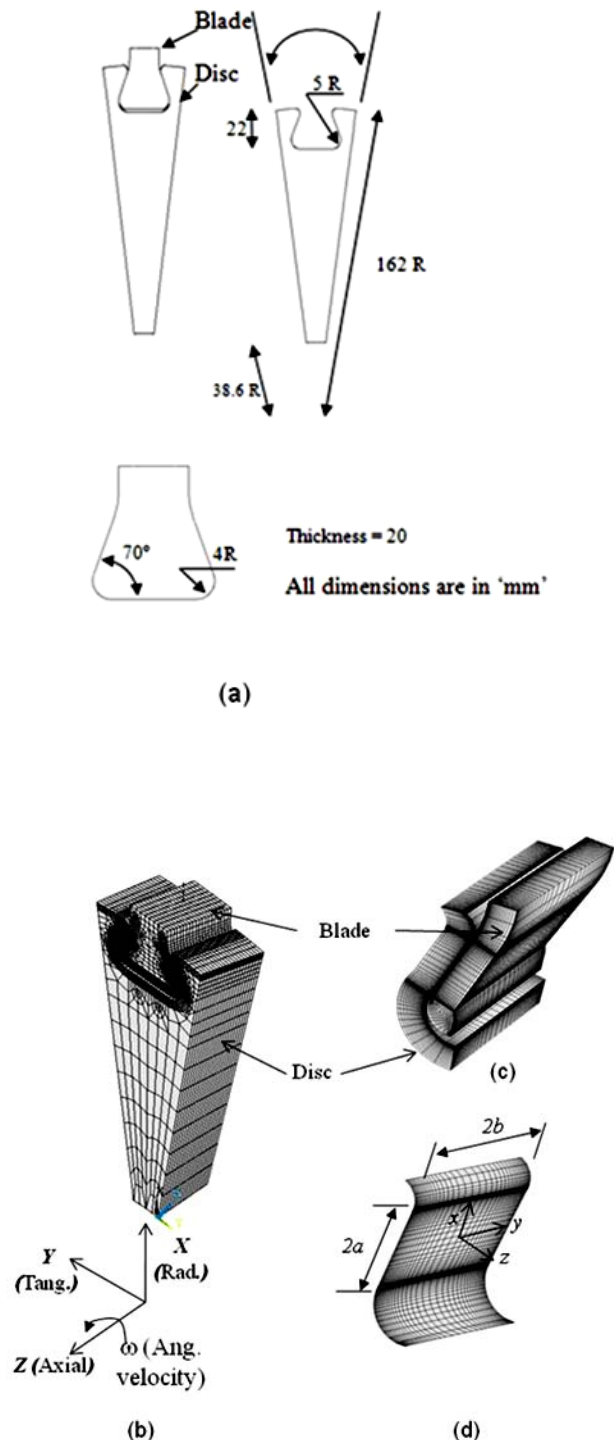

(a)

(b)   (c)   (d)

Fig. 1 Details of (a) Geometry (b) Global FE model, (c) Sub-model mesh, and (d) Contact element at interface

TABLE I
COMBINATION OF LOADS

Load cases (LC)	Interference fit (micrometer)	Angular velocity (rad/sec)
1	0	0
2	5	0
3	15	0
4	25	0
5	50	0
6	0	1050
7	5	1050
8	15	1050
9	25	1050
10	50	1050

III. RESULTS AND DISCUSSION

The macroscopic fretting variables such as contact traction, slip levels and contact stresses at the interfaces are evaluated to understand the preloading effects. The results are discussed for one of the interface, since both interface shows anti-symmetry results pattern, for the load cases studied here.

A. Contact pressure

The contact pressure (normal contact traction) distribution results are presented here. The shear traction distribution is similar to the contact pressure distribution with values equivalent to friction times contact pressure, since gross sliding is observed for the friction coefficient (0.3) considered in this study.

Results of load case-1 show negligible (almost zero) pressure over the interface as the contacts are just established and neither interference load nor bulk is applied. Fig. 2 shows the contact pressure variation over the interface for load cases: 6, 3 and 8. Fig. 2(a) shows the contact pressure developed due to bulk load and zero interference fit. Two peak pressures are observed; one at bottom contact edge (x/a=-1) and other at top contact edge (x/a=1). The highest peak contact pressure occurs at the bottom contact edge and the next peak at the top contact edge. The difference between two peak pressures is significant. The pressure distribution developed for a preload case (interference fit of 15 micrometer) without bulk load and with bulk load is shown in Fig. 2(b) and Fig. 2(c) respectively.

Though the interference fit produces the pressure distribution pattern similar to that observed in pure bulk loading case without preload, the following effects to be noted. The first peak contact pressure is observed at the top contact edge for pure interference fit loading. The preloading also reduces the sharp pressure gradient at the bottom contact

edge of interface. Comparison between Fig. 2(a) and 2(c) clearly shows that the interference fit reduces the magnitude of peak pressure at bottom contact edge up to 35% and increases the top contact edge peak pressure by 58%. Effectively, the peak contact pressure over the interface and the difference between two peak pressures are minimized by the preloading at the interface.
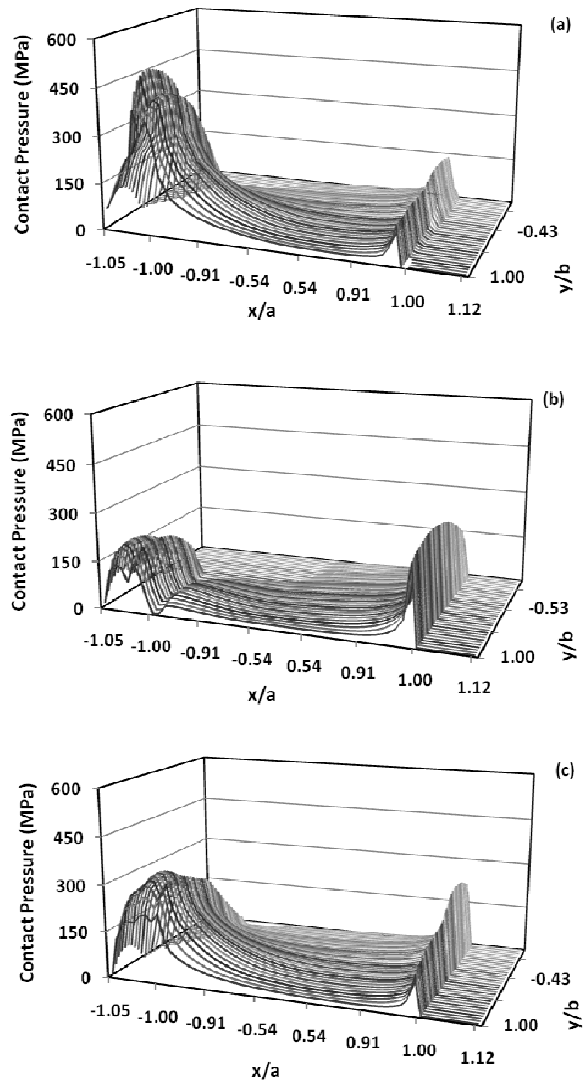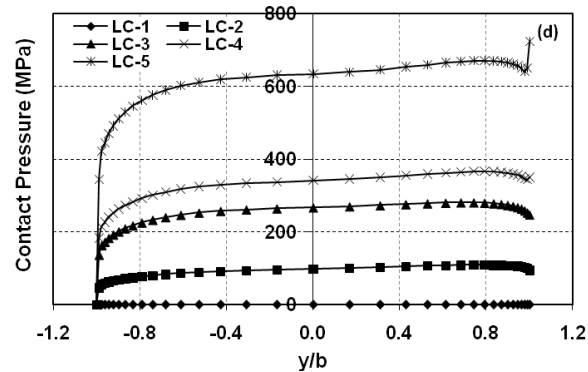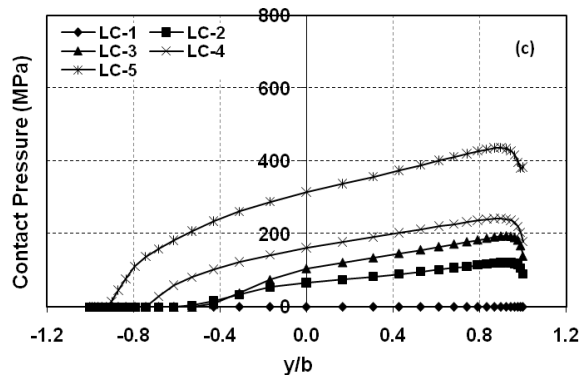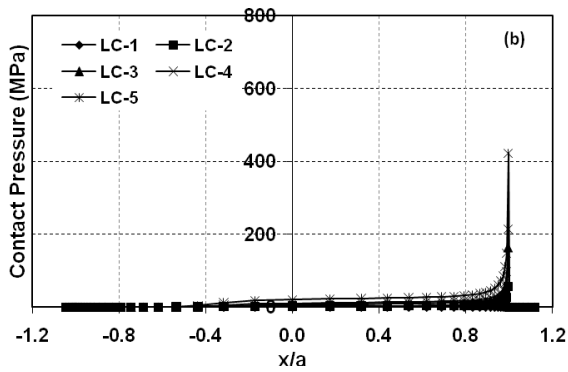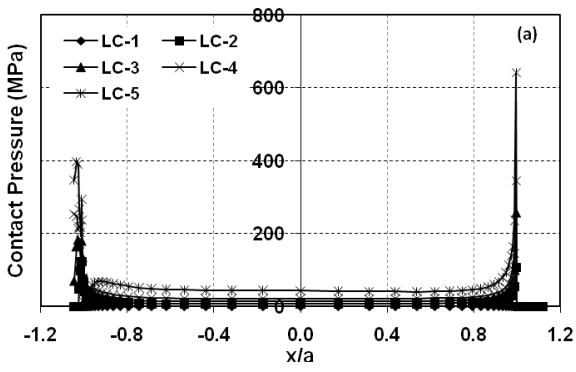

Fig. 2 Contact pressure distribution for (a) Zero fit with bulk load, (b) Interference fit of 15 micrometer without bulk load, and (c) Interference fit of 15 micrometer with bulk load

Fig. 3 shows the contact pressure variation along x (at y/b= -0.98 and 0.98) and along top and bottom contact edges for the different preloading without bulk load. The peak pressure occurs at top contact edges for the pure preload application. The contact pressure variation along the axial direction is less at the top contact edge, while pressure variation is from zero to peak at the bottom contact edges. The contact pressure over the interface increases with increase in preloading.

Contact pressure variation along x (at y/b= -0.98 and 0.98) and top and bottom contact edges, for the bulk loading combined with preloading is shown in Fig. 4. The peak pressure occurs at bottom contact edges for the combined bulk and preload application. The pressure variation along top and bottom contact edges is similar to that observed for no-preload case. The contact pressure decreases with increase in preload of up to 30 micrometer interference fit, and the reverse trend is observed for the interference fit of more than 30 micrometer, for the bottom contact edge. The contact pressure increases with increase in preload, for the top contact edge.
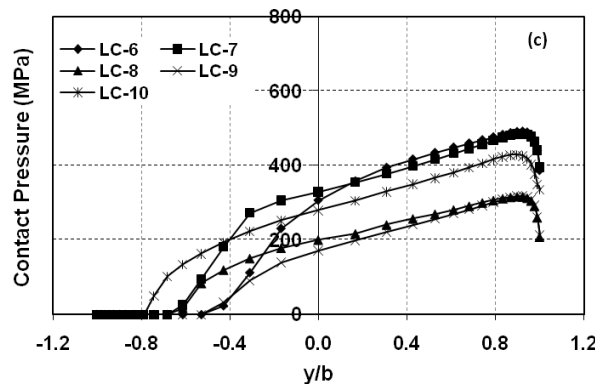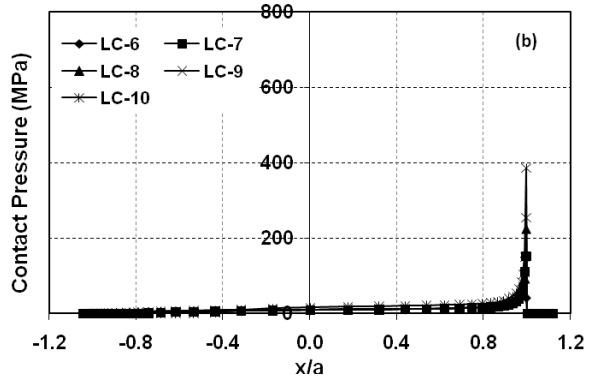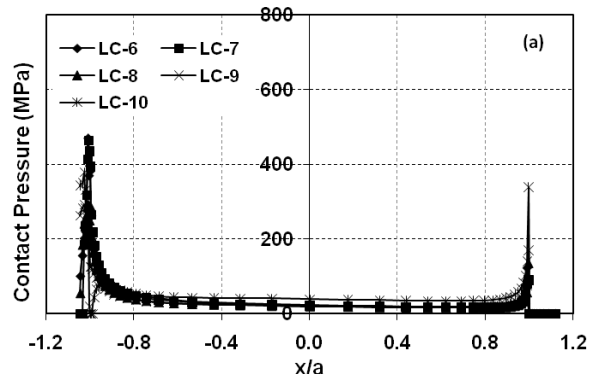
Fig. 3 Contact pressure variation, for different interference fit without bulk load, along (a) y/b=-0.98, (b) y/b=0.98, (c) x/a=-1 and (d) x/a=1
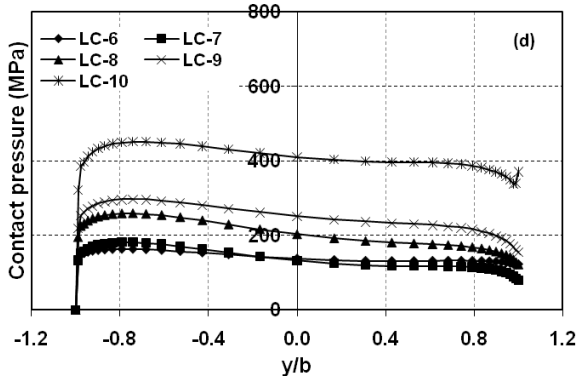
938

Fig. 4 Contact pressure variation, for different interference fit with
bulk load, along (a) y/b=-0.98, (b) y/b=0.98, (c) x/a=-1, (d) x/a=1

Peak contact pressure observed at the top and bottom contact edges are summarized in Table II, for all the load cases studied. The results indicate the peak contact pressure over interface increases with increase in contact load due to only interference fit. The effect of interference fit on the contact pressure, due to bulk load combined with interference fit, is shown in Fig. 5. The results indicate the peak contact pressure over the interface decreases with increase in interference (up to 15 micrometer), and shows the reverse trend for the fit higher than 15 micrometer. The reverse trend is due to the dominant effect of contact pressure developed by higher interference fit.

TABLE II
EFFECT OF INTERFERENCE FIT ON CONTACT PRESSURE

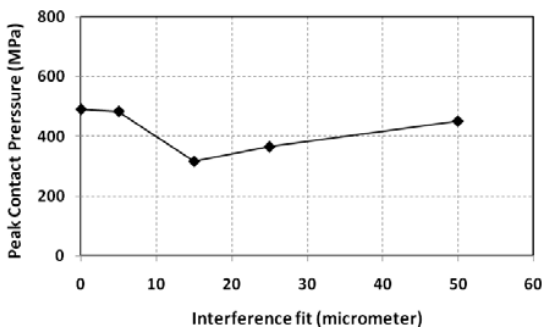| Interference fit (micrometer)	Peak Contact pressure (MPa)			
	Bottom Contact edge		Top contact edge	
	Fit load	Fit + Bulk load	Fit load	Fit + Bulk load
0	0	491	0	163
5	122	484	109	181
15	192	316	280	258
25	254	317	365	296
50	437	429	723	451

Fig. 5 Effect of preload on contact pressure

B. Contact slip level

Fig. 6 shows the effect of preloading on the distribution of slip level at the dovetail interface. The contact separation is indicated by the sudden fall of slip level to zero. Fig. 6(a) indicates contact separation occurs at a corner of the interface (zone x/a< -0.5 and y/b<0) when it is subjected to bulk load without any preloading. The contact separation effect could also be noted in contact pressure distribution plot. The preload application at the interface tries to maintain the contact at the interface as shown in Fig. 6(b). More slip is observed for the bulk load case without preload, when compared to combined bulk load and preload.
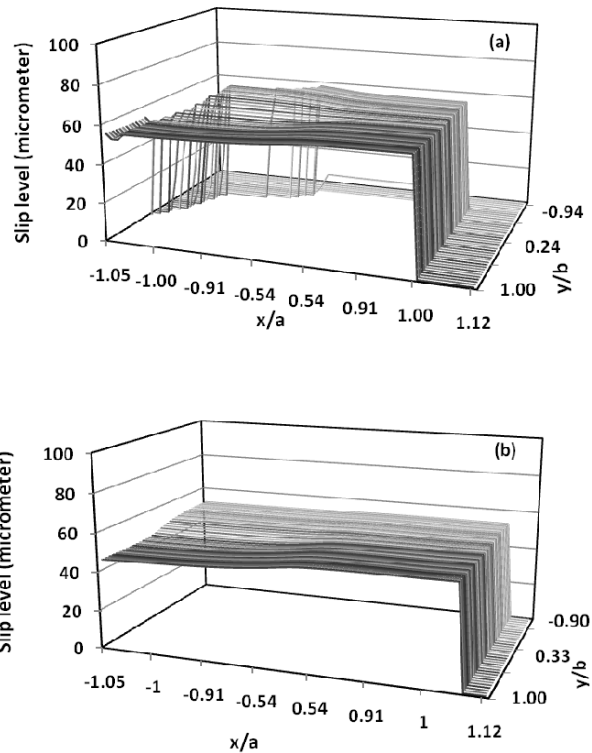

Fig. 6 Distribution of slip level for (a) Bulk load with no preload (b)
Bulk load with interference fit of 15 micrometer.

C. Contact stress

The contact edge stress variation over the interface follows the distribution pattern similar to that of contact pressure distribution shown in Fig. 2. The contact stress plays significant role in the fretting damage at the dovetail interface. The peak contact stresses are observed near the bottom and top contact edges of blade and disc. Fig. 7 shows the effect of different preloading on the peak contact stress over blade and disc at the interface zone. The results indicate the increase in interference fit will reduce the amplitude of cyclic loading stress at the top and bottom contact edge of interface.
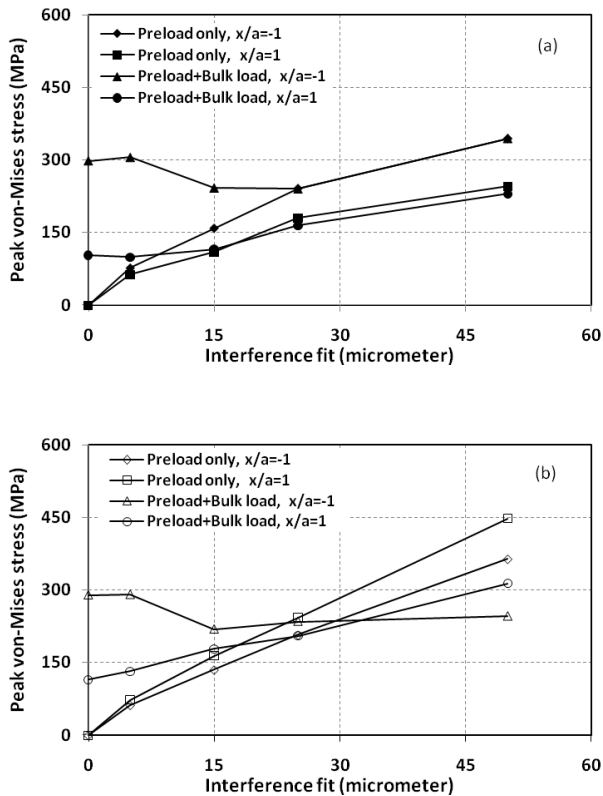
Fig. 7 Effect of interference fit on peak contact stress over (a) disc contact edges and (b) blade contact edges.

IV. CONCLUSION

The preloading at the dovetail interface reduces the peak contact pressure developed due to bulk loading up to 35%. The preloading effect tends to redistribute the contact pressure evenly and this leads to reducing the peak contact pressure and stress difference between top and bottom contact edges. The increase in preloading reduces the cyclic stress amplitude at the interface and hence one could expect an improvement in fatigue life. However the preload also increases the mean stress. Preloading at the interface also brings down the level of the slip between the blade and disc at the interface and would also minimize the fretting damage due to vibratory loads and wind milling effect caused during the engine off condition. The manufacturing and assembly process needs to be established to introduce the preloading by interference, without causing any structural damage, to make use of the benefits of preload effect observed in this study. Further study on the effect of different friction coefficients at the interface, with interference fit, is suggested.

ACKNOWLEDGMENT

REFERENCES

[1] N. S. Xi, P. D. Zhong, H. Q. Huang, H. Yan and C. H. Tao, "Failure investigation of blade and disc in first stage compressor", *Engineering Failure Analysis*, vol. 7, pp. 385–392, 2002.
[2] J. C. Gautreau, N.F. Martin, and C. A. Rickert, "Compressor blade with dovetail slotted to reduces stress on the airfoil leading edge", *Patent No. US7121803B2*, October 17, 2006
[3] J. C. Przytulski and M. C. Hemsworth, "Apparatus for preloading an airfoil loading in a gas turbine engine", *Patent No. US5123813*, June 23, 1992.
[4] C. T. Tsai and Shankar Mall. "Elasto-plastic finite element analysis of fretting stresses in pre-stressed strip in contact with cylindrical pad", *Finite Elements in Analysis and Design*, vol. 36, pp. 171-187, 2000.
[5] P. H. B. Boddington, K.C. Chen and C. Ruiz, "Numerical stress analysis of dovetail joints", *Journal of Computers and Structures*, vol. 2(4), pp. 731-735, 1985.
[6] C. Ruiz, P. H. B. Boddington and K.C. Chen, "An investigation of fatigue and fretting in a dovetail attachment", *Experimental Mechanics*, pp. 208-217, 1984.
[7] S. A. Meguid, M. H. Refaat and P. Papanikos, "Theoretical and experimental studies of structural integrity of dovetail joints in aero engine discs", *Journal of Material Technology*, vol. 56, pp. 1539-1547, 1996.
[8] G. B. Sinclair, N.G. Cormier, J. H. Griffin and G. Meda, "Contact Stresses in dovetail attachments: Finite element modeling", *J. Engng. Gas Turbine Power*, vol. 124, pp. 182-189, 2002, 124.
[9] M. M. I. Hammouda, R. A. Pasha, and A. S. Fayed "Modelling of cracking sites/development in axial dovetail joints of aero-engine compressor discs", *International Journal of Fatigue*, vol. 29, pp. 30-48, 2007.
[10] P. Papanikos, S. A. Meguid, and Z. Stjepanovic, "Three dimensional nonlinear finite element analysis of dovetail joints in aero engines disc", *Finite Element in Analysis and Design*, vol. 29, pp. 668-677, 1998.
[11] J. R. Beisheim, and B. G. Sinclair, "On the three-dimensional finite element analysis of dovetail attachments", in *Proc. of ASME TURBO EXPO 2002*, Amsterdam, The Netherlands, 3-6 June 2002, pp. 1-11.
[12] R. B. Waterhouse, *Fretting Fatigue*, Applied science publishers Ltd., London
[13] ANSYS 11.0 Users Documentation, 2007.
[14] Peter Wrigger, *Computational Contact Mechanics*. The Netherlands: Springer, 2006.